



## Scientific Research

### Investigation of Physicochemical and Rheological Properties of Nanocomplexes Prepared from Sodium Caseinate and Balangu Seed Gum

Roghayeh Ezzati<sup>1</sup>, Leila Roozbeh Nasiraei<sup>1</sup>, Sara Jafarian<sup>1</sup>, Masoud Dezyani<sup>2</sup>, Fatemeh Shahdadi<sup>3</sup>

1- Department of Food Science, Nour Branch, Islamic Azad University, Nour, Iran

2- Department of Food Science, Gorgan Branch, Islamic Azad University, Gorgan, Iran

3- Department of Food Science, Faculty of Agriculture, University of Jiroft, Jiroft, Iran

ARTICLE INFO	ABSTRACT
<p><b>Article History:</b></p> <p>Received: 2025/10/11</p> <p>Review: 2025/12/02</p> <p>Accepted: 2025/12/05</p>	<p>The aim of this study was to prepare and determine the properties of biopolymer nanocomplexes containing sodium caseinate and Balangu seed gum. To produce the nanocomplex, 0.5% sodium caseinate and 0, 0.25 and 0.5% Balangu gum were used. Three types of complexes with different concentration of Balangu gum produced were investigated in terms of turbidity, particle size, zeta potential, as well as shear stress and viscosity and fitting of rheological data. The results showed that the complex of sodium caseinate and 0.5% Balango gum was selected as the better complex. In addition, the effect of the type of homogenizer (single-stage, two-stage and 2-pass) and the homogenization pressure (300, 500 and 700 bar) at pH 3-8 on the turbidity of the complex was investigated and according to the results, the lowest turbidity was for the sample homogenized at 500 bar pressure, pH 3 and 2-pass homogenizer. The selected pH was considered to be 3.5 and the sample at pH 3.5 was affected by the type and pressure of the defined homogenizer and its characteristics were investigated. According to the results, the lowest turbidity (absorption) was related to the sodium caseinate and balangu gum complex sample subjected to double-pass homogenization and 500 bar pressure (0.48). The highest negative zeta potential was related to the sample subjected to double-pass homogenization at 700 bar pressure (-33.35 mV). The lowest particle size was related to the sample subjected to double-pass homogenization at 700 bar (396.66 nm). In all cases studied, the <math>r^2</math> value was high and the RMSE value was low, which indicates pseudoplastic behavior in the complex samples.</p>
<p><b>Keywords:</b></p> <p>Nanocomplex, Balango gum, Sodium caseinate, Rheological properties, Homogenization.</p> <p><b>DOI:</b> 10.48311/fsct.2026.116950.82884</p> <p>*Corresponding Author E-</p>	

## 1- Introduction

In recent years, the use of biopolymer nanoparticles in food and pharmaceutical systems as an encapsulation agent for bioactive compounds and nutraceuticals (such as vitamins, carotenoids, essential fatty acids, flavonoids, sterols, etc.) has received much attention and has found many applications in drug delivery and delivery systems for targeted delivery. Nanoparticles are produced either alone by assembling and joining chains of a single type of biopolymer (protein or polysaccharide) or by controlling the binding and complexation of protein and polysaccharide molecules. Protein-polysaccharide nanocomplexes have attracted more attention than pure biopolymer nanoparticles due to their higher chemical and colloidal protection [1].

Paying attention to various microencapsulation systems and finding new, inexpensive, and effective compounds in this field and creating functional food compounds can be a way to achieve healthier nutrition and ultimately ensure the health of the community. The use of new wall compounds that, in addition to affecting product characteristics, have functional, inexpensive, and available properties will be considered in this research. Granular mucilages and plant polysaccharides are in this category. Balangu, with the scientific name *Lallemantia royleana*, is a glazed plant from the mint family that grows in different regions of the world, especially in the Middle East. The seed of the Balangu is an elongated oval-shaped plant that can be cultivated and harvested in Asia and Northern Europe. If soaked in water, the Balangu seed produces a viscous, cloudy, and tasteless liquid (mucilage). Due to the production of high amounts of mucilage, this seed can be used as a new source of hydrocolloid in the food industry for various purposes [2]. The gum of the Balangu seed contains 61.74% carbohydrates, 0.87% protein, 29% crude fiber, and 33.8% ash [3].

Sodium caseinate is the sodium salt of casein, which has a pleasant taste and, due to its ability to form extensive intermolecular hydrogen bonds, can easily form aqueous solutions. This substance is highly soluble and disperses very quickly in an aqueous mixture and also becomes homogeneous in the presence of oil and fat. Casein coatings and films are used as microencapsulating agents for flavor, drugs, fruit and vegetable coatings, and cheese. Sodium caseinate can easily form a film from an aqueous solution. Due to the structure of casein and its amino acid sequence, hydrogen bonds, electrostatic interactions, and hydrophobic forces, it is effective in film formation [4].

The formation of electrostatic complexes between sodium caseinate and gums such as balangu allows the development of stable drug delivery systems. These complexes help in the encapsulation of sensitive compounds and provide favorable rheological properties to dairy matrices [5].

Research has shown that the use of natural biopolymers such as sodium alginate, chitosan, tragacanth gum, arabic gum, and maltodextrin, depending on the type of target compound, wall matrix characteristics, processing method, and environmental conditions, has a significant impact on encapsulation efficiency, composition stability, and release behavior [1]. Finally, although modern technologies have been successful in increasing the efficiency and stability of microencapsulation, challenges such as safety, sensitivity to environmental conditions, and industrialization of these technologies still exist, and further research is needed at the applied and clinical levels. In this study, the high-pressure homogenization method was used to produce nano emulsions; a method that has been used in numerous studies for different nanostructures, but its effect on the system containing the complex of balangu gum and sodium caseinate protein has not been investigated so far. Therefore, the aim of this study was to optimize the

preparation of this complex and evaluate its physicochemical properties before and after applying high pressure.

## 2-Materials and Methods

The chemicals used in this study included sodium caseinate (Sigma, New Zealand), sodium hydroxide (Merck, Germany), and hydrochloric acid (Merck, Germany). The Shirazi balangu used in this study was purchased from traditional Tabriz perfume shops. After grinding with a grinder (Sanyo, Japan) and passing through a laboratory sieve with a mesh size of 60, the resulting powder was stored in a cool, dry place for experiments.

### 2-1- Preparation of the balangu and sodium caseinate solutions

The desired amount of balangu powder was added to distilled water and the mixture was stirred for 12 h by a magnetic stirrer (IKA-MAG HS 7, Germany) at 4000 rpm to absorb water and create a uniform texture. After heating in a hot water bath for 10 min (to help absorb water) at a temperature of 70 °C, it was stored at refrigerator temperature for 12 h to complete the water absorption process [6].

Sodium caseinate powder was also added to distilled water and after 30 min of mixing by a magnetic stirrer, it was stored overnight at 4 °C to ensure complete dissolution and dehydration [7].

### 2-2- Preparation of nanocomplex of balangu and sodium caseinate

The optimum pH for hydrogel formation was determined by measuring the zeta potential of solutions of balangu gum and sodium caseinate as a function of pH in the range of pH = 3-8. The pH was adjusted using a solution of soda and acid [9]. Then, sodium caseinate (0.5%) and balangu solution were mixed together in different ratios (0, 0.25 and 5%) and after adjusting the pH to the optimum

level for preparing the nanocomplex, the resulting mixture was passed through a high-pressure homogenizer (HST-15DA366, Germany). The effect of pressure on the formation of nanohydrogel was investigated at two levels and its particle size, rheological properties, zeta potential, stability and turbidity were measured and the chemical bonds formed were determined using Fourier transform infrared spectroscopy (FTIR).

### 2-2- Evaluation of physicochemical properties

#### Turbidity measurement

Complete mixing of the samples was done using a high-speed mixer before measurement. The turbidity of the nanocomplex mixture was measured using a UV-Visible spectrometer (T85, Iran) as a function of pH in the range of 3-8 [8].

#### Particle size measurement

The particle size distribution and their average diameter were measured in a Zeta Sizer (Nano-ZS, Malvern, UK) [9].

#### Zeta potential measurement

A Zeta Sizer (Nano-ZS, Malvern, UK) was used to determine the zeta potential of the samples. The method used in this device is to measure the zeta potential using laser Doppler electrophoresis. Electrophoresis refers to the movement of charged particles in a suspension under the influence of an applied electric field. Therefore, if a diluted colloidal suspension is exposed to an electric field and a laser beam is passed through the sample at the same time, the charged particle and ions located in the suspension move towards the electrode with the opposite electric charge. In this way, by obtaining the particle velocity, the electrophoretic mobility can be calculated. Finally, based on the defined relations, it is possible to establish a relationship between the electrophoretic mobility and the zeta potential. In order to measure the zeta potential, each of the samples was first diluted

100 times using distilled water. Then, the samples were transferred into the capillary tube (cell) using a syringe and the capillary tube was placed in the installed location inside the device. The zeta potential was measured at ambient temperature (25 ° C) and a power of 149 watts. Finally, the zeta potential was calculated by the device itself according to the relevant relations and reported as a pure number [6].

#### 2-4- FTIR spectroscopy

Fourier transform infrared is a method that can be used to identify and investigate the chemical structure of molecules. The position, shape and intensity of the peaks obtained from the FTIR curve show details about the molecular structure of the sample. An FTIR device (Agilent technologies Cary 360, USA) was used to measure the IR spectrum. A small amount of the sample (in solid or liquid form depending on the type of sample) was placed on the lens of the device and the resulting spectrum was examined in the wavenumber range of 400-4000 cm<sup>-1</sup> with a resolution of 1-4 cm in the FTIR device [10].

#### 2-5- Investigation of rheological properties

A rheometer (Anton Paar- Rheolab QC, Germany) was used to measure the shear stress and viscosity as a function of shear rate and to determine the type of flow behavior of the samples. To determine and predict the flow behavior under different conditions, the fit of the data obtained from practical tests with Newtonian, power law, Bingham, Herschel-Bulkeley, and Sisko models was evaluated. Then, the most appropriate mathematical model was selected based on the coefficient of determination indices r<sup>2</sup>, RMSE and  $\chi^2$  and finally the rheological indices for each of the samples were reported [6]. The data were fitted with Matlab software.

Eq. (1): Newtonian model

$$\sigma = \eta \dot{\gamma}$$

$\sigma$  = shear stress (Pa),  $\eta$  = viscosity (Pa.s) and  $\dot{\gamma}$  = shear rate (s<sup>-1</sup>).

Eq. (2): Bingham model

$$\sigma = \eta \dot{\gamma} + \sigma_0$$

$\sigma$  = shear stress (Pa),  $\eta$  = viscosity (Pa.s) and  $\dot{\gamma}$  = shear rate (s<sup>-1</sup>) and  $\sigma_0$  = yield stress.

Eq. (3): Power law model

$$\sigma = k \dot{\gamma}^n$$

$\sigma$  = shear stress (Pa), k = consistency index (Pa.sn), n = power law index and  $\dot{\gamma}$  = shear rate (s<sup>-1</sup>).

Eq. (4): Herschel-Bulkeley model

$$\sigma = k \dot{\gamma}^n + \sigma_0$$

$\sigma$  = shear stress (Pa), k = consistency coefficient (Pa.sn), n = quasi-plastic constant,  $\dot{\gamma}$  = shear rate (s<sup>-1</sup>) and  $\sigma_0$  = yield stress (Pa).

Eq. (5): Sisco model

$$\sigma = k \dot{\gamma}^n + \eta_{\infty} \dot{\gamma}$$

$\sigma$  = Shear stress (Pa), k = Consistency index (Pa.sn), n = Power law index,  $\dot{\gamma}$  = Shear rate (s<sup>-1</sup>) and  $\eta_{\infty}$  = Infinite viscosity (Pa).

### 3-Results and Discussion

#### 3-1-Effect of pH and concentration of balangu gum on the phase behavior of sodium caseinate solution (0.5%)

The effect of pH and concentration of gum balangu on the phase behavior of sodium caseinate solution (0.5%) is shown in Table 1.

**Table 1- Effect of pH and concentration of balangu gum on the phase behavior of sodium caseinate solution (0.5%)**

Balangu concentration	pH	phase behavior
0	3	Solution
0.25	3	Precipitation with clear solution
0.5	3	Precipitation with cloudy solution
0	4	Solution
0.25	4	Cloudy/milky solution
0.5	4	Cloudy/milky solution
0	5	Precipitation with clear solution
0.25	5	Cloudy/milky solution
0.5	5	Cloudy/milky solution
0	6	Solution
0.25	6	Solution
0.5	6	Solution
0	7	Solution
0.25	7	Solution
0.5	7	Solution
0	8	Solution
0.25	8	Solution
0.5	8	Solution

According to the results of Table 1, with increasing pH, the phase behavior of the complex containing sodium caseinate and balangu gum moves towards greater solubility. At acidic pHs, the solution is almost cloudy in all complexes, and by adding balangu gum to the complex, a cloudy and milky solution is obtained. Precipitation occurs mainly at isoelectric pHs, the isoelectric pH range of caseinate, which is an insoluble protein, is between 4 and 5. At isoelectric pH, aggregation and precipitation are observed due to the equalization of the positive ( $\text{NH}_3^+$ ) and negative ( $\text{COO}^-$ ) charges of the protein and the creation of electrostatic attraction between the unlike charges. At pHs higher and lower than the isoelectric point, the dominance of negative and positive charges, respectively, and the presence of electrostatic repulsion prevent the protein particles from approaching each other, and as a result, a clear

solution without precipitation is observed [12, 11, 1].

According to the results, at pH 3, increasing the amount of balangu gum to 0.25% results in a cloudy solution, and adding more balangu gum results in a cloudy precipitate. Sodium caseinate without balangu gum also formed a precipitate only at pH 5, which is close to the isoelectric point. Balangu gum is polysaccharide in nature and forms a milky solution complex at pH 5 when mixed with sodium caseinate. Jourdain et al. investigated the complex of sodium caseinate and dextran gum and reported that the precipitate formed at pH 3.5 to 5 at low polysaccharide concentrations is related to the normal precipitation of sodium caseinate around the isoelectric pH of the protein, and the precipitate formed at pH 2 to 3.5 indicates the formation of an insoluble complex due to the strong attraction between the two biopolymers by opposite charges [13].

### 3-2- The average turbidity of the nanocomplex of sodium caseinate (0.5%) and gum balangu under the influence of pH

The results of the average turbidity of the nanocomplex of sodium caseinate (0.5%) and balangu gum under the influence of pH and gum balangu concentration are shown in Table 2.

**Table 2 - Turbidity of sodium caseinate nanocomplex (0.5%) and balangu under the influence of pH and balangu gum concentration**

Sample \ pH	T1	T2	T3
3	0.25±0.01 <sup>Fe</sup>	0.5±0.03 <sup>Dc</sup>	0.55±0.01 <sup>Bbc</sup>
4	0.30±0.02 <sup>EFde</sup>	0.65±0.02 <sup>ABab</sup>	0.70±0.02 <sup>Aa</sup>
5	0.50±0.02 <sup>Dc</sup>	0.5±0.03 <sup>Dc</sup>	0.55±0.03 <sup>CDbc</sup>
6	0.35±0.03 <sup>Ed</sup>	0.55±0.01 <sup>CDbc</sup>	0.60±0.02 <sup>Bb</sup>
7	0.30±0.01 <sup>EFde</sup>	0.5±0.03 <sup>Dc</sup>	0.55±0.01 <sup>CDbc</sup>
8	0.25±0.02 <sup>Fe</sup>	0.55±0.02 <sup>CDbc</sup>	0.60±0.01 <sup>Bb</sup>

T1: Sodium caseinate nanocomplex and 0% balangu gum, T2: Sodium caseinate nanocomplex and 0.25% balangu gum, T3: Sodium caseinate nanocomplex and 0.5% balangu gum

Different lowercase letters in each row indicate significant differences between samples with different balangu concentrations and different uppercase letters in each column indicate significant differences at different pHs ( $p \leq 0.05$ ).

Turbidity measurements were performed to investigate the effect of changing the protein-polysaccharide ratio on complex formation and to find the optimal pH for complex formation. Any significant change in absorption should reveal the appearance of coacervates or aggregates by changing the optical properties of the system. Turbidimetric measurements have been widely used to monitor the complex coacervation process in various protein-polysaccharide systems [14]. According to the results in Table 2, there is a statistically significant between the turbidity of the sodium caseinate and gum balangu nanocomplexes, considering the gum concentration used in the complex ( $p < 0.05$ ), and with increasing the gum balangu concentration in the complex, regardless of the pH, the turbidity of the complex increases, such that the highest turbidity at each pH corresponds to the complex containing 0.5% gum balangu. Regarding the pH, the sample without balangu gum had the highest turbidity at pH 5 and the lowest turbidity at pH 3, and

the highest turbidity in the complex containing 0.25 and 0.5 % of balangu gum was related to pH 4. Therefore, considering the pH values studied in each sample with different percentages of balangu gum, which is a polysaccharide-containing system, the turbidity increases with increasing pH. In sample T1, the sodium caseinate complex without balangu gum has the lowest turbidity at pH 8. Considering that initially in the complexes under study, turbidity increased with increasing pH and then decreased again, it can be concluded that the solubility of sodium caseinate is a function of pH [15]. The turbidity was obtained based on the amount of absorption, and the maximum absorption can be related to the aggregation of particles due to the presence of attractive forces, van der Waals forces, and electrostatic forces. There is always the possibility of protein binding to polysaccharides via  $N+R_3$  and  $-CSO_3^-$  or  $-COO^-$  groups [9]. It is assumed that the decrease in turbidity is the result of large-scale aggregation and subsequent precipitation of

caseinate samples. The aggregation of sodium caseinate may occur due to the reduction of electrostatic repulsion between proteins around their  $pI=4.6$ . Also, further acidification can create more positive charges on caseinate, which can lead to an increase in protein solubility and consequently a decrease in turbidity of the system [16].

The adsorption of sodium caseinate and balangu gum showed a different profile than sodium caseinate alone (T1), indicating an interaction between protein and polysaccharide. The addition of gum to the sodium caseinate solution caused a significant increase in the initial turbidity increase, which

could be related to the weak association of sodium caseinate with balangu gum at higher pH levels through hydrophobic interactions [17]. Although at higher pH, sodium caseinate did not reach its  $pI$ , its molecules may have positive points while the overall charge on the caseinate molecules is negative [18].

According to the results, the optimum pH for the sodium caseinate and balangu gum nanocomplex was considered to be 3.5 and the absorption at pH 3.5 was measured to investigate the turbidity. The results of the comparison of the average turbidity values of the complexes are shown in Table 3.

**Table 3-Turbidity of sodium caseinate nanocomplex (0.5%) and balangu gum at pH 3.5**

Treatment	Turbidity
T1	0.55±0.02 <sup>c</sup>
T2	0.60±0.05 <sup>b</sup>
T3	0.66±0.03 <sup>a</sup>

T1: Sodium caseinate nanocomplex and 0% balangu gum, T2: Sodium caseinate nanocomplex and 0.25% balangu gum, T3: Sodium caseinate nanocomplex and 0.5% balangu gum

According to the results in Table 3, there is a statistically significant difference ( $p<0.05$ ) between the turbidity (absorption) of sodium caseinate (T1) and the samples containing 0.25 and 0.5 percent of balangu gum. The highest absorption and turbidity are related to the sample containing 0.5 percent of balangu gum. The results show that some attractive electrostatic interactions have occurred between sodium caseinate and balangu gum.

**Table 4- Particle size of sodium caseinate nanocomplex (0.5%) and balangu gum at pH 3.5**

Treatment	Particle size (nm)
T1	1.00±0.05 <sup>a</sup>
T2	0.90±0.02 <sup>b</sup>
T3	0.95±0.03 <sup>c</sup>

T1: Sodium caseinate nanocomplex and 0% balangu gum, T2: Sodium caseinate nanocomplex and 0.25% balangu gum, T3: Sodium caseinate nanocomplex and 0.5% balangu gum

According to the results of Table 4, there is a statistically significant difference between the particle size of sodium caseinate (T1) and the samples containing 0.25 and 0.5 % of balangu gum (T2 and T3) ( $p<0.05$ ). The largest particle size is related to the sample containing sodium

### 3-3- Particle size of sodium caseinate nanocomplex (0.5 %) and balangu gum

The particle size of sodium caseinate nanocomplex (0.5 %) and balangu gum is shown in Table 4.

caseinate and the smallest particle size is related to the sample containing 0.25 % of balangu gum. The greater the amount of aggregation, the larger the particle size will be. Although aggregation is also related to the pH level, the optimal pH in this study is

considered to be 3.5, and this pH is lower than the isoelectric point of sodium caseinate; therefore, considering the isoelectric point of sodium caseinate, which is equal to 4.6, it is far from its isoelectric point and has fewer aggregations because a further decrease in pH creates more positive charges on caseinate and due to repulsive forces, large aggregations become smaller aggregations. As a result, the solubility of the protein increases and the number of insoluble protein particles decreases. This phenomenon explains why the particles are smaller at pH 3.5. The smallest particles were observed in the complex containing 0.25% of balangu gum. The reduction in the size of the complex particles may be due to the contraction of the molecule, which expands less when sodium caseinate interacts with the carboxylic groups of the polysaccharide, leading to a decrease in intermolecular repulsion [14]. It is clear that the particle size of the sodium caseinate-balangu gum complexes is strongly affected by the presence of the gum. Furthermore, these results show that at this pH, the presence of sodium caseinate leads to the formation of nanoparticles that are even smaller than the bare sodium caseinate particles. The decrease

**Table 5- Zeta potential of sodium caseinate nanocomplex (0.5%) and balangu gum at pH 3.5**

Treatment	Zeta potential (mV)
T1	6.66 <sup>a</sup>
T2	-5.33 <sup>b</sup>
T3	-7.33 <sup>c</sup>

T1: Sodium caseinate nanocomplex and 0% balangu gum, T2: Sodium caseinate nanocomplex and 0.25% balangu gum, T3: Sodium caseinate nanocomplex and 0.5% balangu gum

To determine the action of electrostatic repulsive forces in the gum-sodium caseinate complex and the stability of the resulting complex, zeta potential results were used. Zeta potential or electrokinetic potential is the potential difference between the mobile and immobile ionic layers and is the best indicator for determining the surface electrical state of dispersions, because it indicates the amount of charge accumulation in the immobile layer and the intensity of adsorption of counterions to the particle surface [21]. Various factors,

in particle size with the addition of 0.25% of gum balangu is due to the strong interactions between sodium caseinate and polysaccharide, which resulted in a relatively compact structure. The particle size continued to increase with increasing gum balangu concentration. This result can be explained by the decrease in electrostatic repulsion between nanoparticles [19].

The results of the present study are also consistent with those of Gorji et al., in which a complex of sodium caseinate and tragacanth gum was produced, and the particle size of the complex decreased with the addition of gum [14]. Karim et al. (2024) also reported a particle size of approximately 17.2 nm for the complex of sodium caseinate and peach gum [20].

### 3-4- Zeta potential of sodium caseinate nanocomplex (0.5%) and balangu gum

The zeta potential of sodium caseinate nanocomplex (0.5%) and balangu gum is shown in Table 5.

including pH, ionic strength, type and concentration of biopolymers used, and the ratio between them, affect the amount of surface charge and zeta potential of the complex.

According to the results in Table 5, there is a statistically significant difference between the zeta potentials of the complex samples ( $p < 0.05$ ). With increasing the amount of balangu gum in the complex, the zeta potential of the samples increases, although it is

negative. In such a way that the sample containing 0.5% of balangu gum has a higher negative zeta potential than the other two samples. At the same concentration of caseinate, with increasing gum content, the negative zeta potential value increased, which can be attributed to the appropriate coating of caseinate. In this case, the negative repulsive force of the particle surface increases and ultimately the negative zeta potential value increases. The results of the present study are consistent with the results of Akrami et al. In the study of these researchers, a complex of sodium caseinate and Arabic gum was prepared [21]. As shown in the table, the effect of pH on zeta potential, like particle size, shows a great dependence on the gum concentration; with a decrease in pH (3.5), the negative charge of the gum structure is reduced due to the protonation of the carboxylic acid groups present in the uronic acids [6]. As previously stated, the formation of a complex occurs between polymers with opposite charges, therefore; According to the results of zeta potential measurements and the difference in surface charge of the two biopolymers used at specific pHs, if the appropriate conditions are selected in terms of pH and the ratio of the two polymers, it will be possible to form a complex without forming a precipitate. Since the net charge of biopolymers is an indication of the electrostatic interaction between them, the net charge of the complexes can be useful in determining the effective mechanism in stability [9].

Zeta potential measurements make it possible to predict the storage stability of colloidal dispersions. High values of zeta potential, whether positive or negative, are required to

ensure stability and non-agglomeration of particles. Theoretically, the higher the zeta potential, the better the interaction between charged compounds will take place [22]. In the presence of caseinate as a protein material, due to the lower amount of protein, the numerical value of zeta potential is higher. With increasing gum concentration, the zeta potential value increased, and considering that high values of zeta potential, both positive and negative, are required for stability [23], it can be concluded that the stability of the complex system will also increase and the formation of two phases and the formation of sediment will decrease or not be observed. In a study, Ye et al. evaluated the zeta potential of a nanocomplex of sodium caseinate and coreless Arabic gum at different pHs and showed that increasing the ratio of Arabic gum to caseinate causes a decrease in the neutralization pH (isoelectric point) of the complex [16]. Rashid et al. investigated the complex of sodium caseinate and peach gum and reported the zeta potential of the complex containing 1% gum to be -21.36 mV [24]. Karim et al. (2024) also reported the zeta potential of the complex of sodium caseinate and peach gum 84/17- reported [20].

### 3-5- Rheological properties of sodium caseinate nanocomplex (0.5%) and balangu gum

#### 3-5-1- Results of shear stress of sodium caseinate nanocomplex (0.5%) and balangu gum against shear rate

The results of shear stress of sodium caseinate nanocomplex (0.5%) and balangu gum with different shear rates are given in Table 6 and Figure 1.

**Table 6- Shear stress (Pa) of sodium caseinate nanocomplex (0.5%) and balangu gum at different shear rates (1/S)**

Sample	T1	T2	T3
Shear rate			
0	1.33±0.2 <sup>Kb</sup>	3.33±0.1 <sup>Ga</sup>	3.66±0.3 <sup>Ba</sup>

100	2.33±0.3 <sup>Hc</sup>	4.33±0.2 <sup>Fb</sup>	5.33±0.3 <sup>Ea</sup>
200	3.33±0.1 <sup>Gc</sup>	4.66±0.4 <sup>Fb</sup>	6.10±0.5 <sup>Da</sup>
300	3.66±0.2 <sup>Gc</sup>	5.10±0.3 <sup>Eb</sup>	6.33±0.2 <sup>Da</sup>
400	4.10±0.5 <sup>Fc</sup>	5.66±0.5 <sup>Eb</sup>	7.33±0.2 <sup>Ca</sup>
500	4.33±0.2 <sup>Fc</sup>	6.10±0.2 <sup>Db</sup>	8.10±0.1 <sup>Ba</sup>
600	4.66±0.5 <sup>Fc</sup>	6.33±0.1 <sup>Db</sup>	9.60±0.2 <sup>Aa</sup>

T1: Sodium caseinate nanocomplex and 0% balangu gum, T2: Sodium caseinate nanocomplex and 0.25% balangu gum, T3: Sodium caseinate nanocomplex and 0.5% balangu gum

Different lowercase letters in each row indicate significant differences between samples with different balangu concentrations and different uppercase letters in each column indicate significant differences at different shear rates ( $p \leq 0.05$ ).

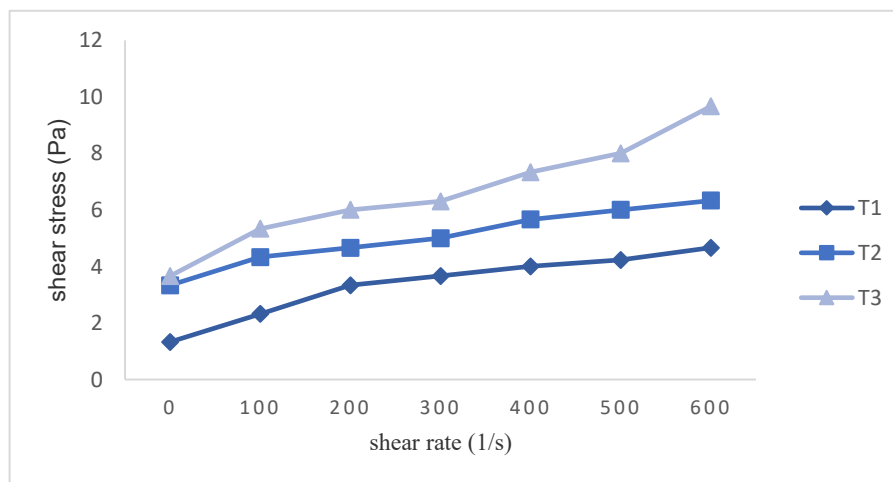


**Figure-1 Shear stress of sodium caseinate nanocomplex (0.5%) and balangu gum at different shear rates**

According to the results of Table 6 and Figure 1, there is a significant difference between the shear stress levels of the complex samples at each applied shear rate ( $p < 0.05$ ). With increasing the amount of balangu gum, the shear stress level increased so that at each applied shear rate, the sodium caseinate sample had the lowest shear stress and the sample containing more balangu gum (0.5%) had the highest shear stress. The shear stress level in the sodium caseinate sample with shear rates of 0 to 600 (1/s) was between 1.33

and 4.66 pa, and in the sample containing 0.25% balangu gum it was between 3.33 and 3.63 pa, and in the sample containing 0.5% balangu gum it was between 3.66 and 9.66 pa.

### 3-5-2- Viscosity of sodium caseinate nanocomplex (0.5%) and balangu gum at different shear rates

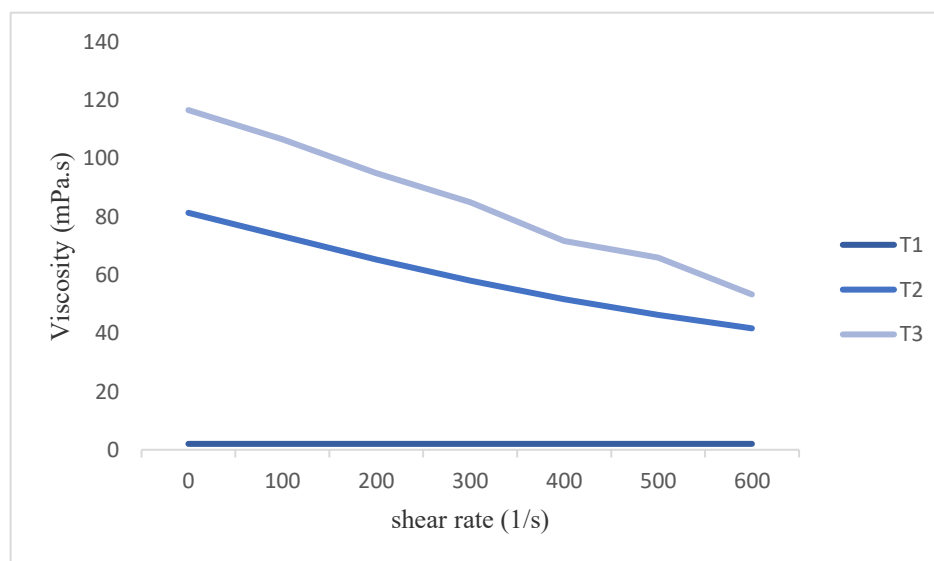
The viscosity of sodium caseinate nanocomplex (0.5%) and gum balangu at different shear rates is shown in Table 7 and Figure 2.

**Table 7- Viscosity (mPa.s) of sodium caseinate nanocomplex and balangu gum at different shear rates**

Sample \ Shear rate	T1	T2	T3
0	2.00±0.2 <sup>Gc</sup>	81.33±1.2 <sup>Cb</sup>	116.15±4.1 <sup>Aa</sup>
100	2.00±0.5 <sup>Gc</sup>	73.33±1.5 <sup>Db</sup>	106.67±3.2 <sup>ABa</sup>
200	2.00±0.1 <sup>Gc</sup>	65.33±2.2 <sup>Db</sup>	95.50±1.6 <sup>BCa</sup>
300	2.00±0.3 <sup>Gc</sup>	58.64±1.3 <sup>DEb</sup>	85.50±1.9 <sup>Ca</sup>
400	2.00±0.2 <sup>Gc</sup>	51.66±1.3 <sup>Eb</sup>	71.20±2.2 <sup>Da</sup>
500	2.00±0.4 <sup>Gc</sup>	46.33±2.1 <sup>EFb</sup>	66.10±2.3 <sup>Da</sup>
600	2.00±0.2 <sup>Gc</sup>	41.66±1.5 <sup>Fb</sup>	53.33±3.1 <sup>Ea</sup>

T1: Sodium caseinate nanocomplex and 0% balangu gum, T2: Sodium caseinate nanocomplex and 0.25% balangu gum, T3: Sodium caseinate nanocomplex and 0.5% balangu gum

Different lowercase letters in each row indicate significant differences between samples with different balangu concentrations and different uppercase letters in each column indicate significant differences at different shear rates ( $p \leq 0.05$ ).

**Figure 2- Viscosity (mPa.s) of sodium caseinate nanocomplex (0.5%) and balangu gum at different shear rates**

According to Table 7, it can be seen that in T1 (sample containing sodium caseinate) there is no significant difference between the viscosity at different shear rates ( $p > 0.05$ ). In samples T2 and T3, with increasing shear rate, the viscosity decreases. With increasing amount of balangu gum, the viscosity increases so that

at each applied shear rate, the sodium caseinate sample has the lowest viscosity and the sample containing more balangu gum (0.5%) has the highest viscosity. The viscosity in the sample containing 0.25 balangu gum is between 33.81 and 66.44 mPas-sec and in the

sample containing 0.5% balango gum is between 67.116 and 33.53 mPas-sec.

There is a relatively linear relationship between shear stress and shear rate in the complex of balango gum and sodium caseinate, and this behavior indicates that the solutions have a behavior close to Newtonian. In these fluids, the slope of the shear stress-shear rate graph indicates viscosity, so that with increasing solution viscosity, the slope of the curve also increases. According to the results of the table, at low shear rates, the samples exhibit shear-fluidity (pseudoplastic) behavior, and with increasing shear rate, the viscosity decreases, which can be attributed to the initial decrease in friction due to the alignment of dispersed phase particles and the dominance of shear force over Brownian force [25]. The presence of balango gum can prevent the coagulation of casein particles and prevent a sharp increase in viscosity by creating repulsive forces due to steric hindrance and electrostatic repulsion. Also, by increasing the gum concentration from 0.25 to 0.5%, the viscosity of the complex solutions increased. If there is a change of state from dilute to semi-dilute in a system, the increase in viscosity can be attributed to the entanglement and trapping of chains, but since in this system, due to the dilution, there is no change of state, the increase in viscosity cannot be attributed to it, but rather the increase in viscosity is likely due to the increase in the number of complex particles and, as a result, increased friction. Another possibility is the increase in particle agglomeration due to the formation of bridges or depletion. At a constant particle volume fraction, the viscosity values of the colloidal system depend on the particle size, particle size distribution, flocculation, and the presence of a thick surfactant layer around the particles. Smaller particles with a narrower size distribution produce higher viscosity, and particle agglomeration due to the entrapment

of the solvent also causes an increase in viscosity [21]. Norouzi et al. used balango gum in yogurt formulation and stated that with increasing the amount of balango gum used in the formulation, the apparent viscosity increases [25].

The formation of a bond between water and balango gum causes an increase in viscosity, and this is because the viscosity increases with increasing the amount of balango gum in the complex. Increasing balango gum strengthens the protein system (caseinate). In fact, the polysaccharide nature of balango gum causes high water absorption and increases viscosity and increases resistance to force. This is because samples with more gum have higher viscosity and after applying shear force, they also have higher viscosity [25].

In their study, Najaf Najafi and Fazeli stated that the slowing down of the Brownian motion of oil particles in the emulsion is the reason for the decrease in the size of emulsion particles with increasing viscosity. They also stated that the reverse is also true, such that emulsions with smaller droplets have higher viscosity than emulsions with larger droplets [26].

### **3-6- Effect of Balangu Gum Concentration on the Fit of Rheological Data of the Complex with Mathematical Models**

In order to achieve a desirable mathematical model that can be used to study the flow behavior of the resulting complexes, the data obtained from the rheological test were examined with Newtonian, power law, Bingham, Herschel-Bulkeley, and Sisko models. The coefficient of determination<sup>1</sup>, root mean square error from the standard<sup>2</sup>, and the sum of squared errors obtained<sup>3</sup> for each of the models are given in Table 8. Basically, the high coefficient of determination and the low RMSE and SSE indicate that the fit of the

---

1-R<sup>2</sup>

2-RMSE: Root Mean Standard Error

3-SSE: Sum of Squares Error

experimental data with the model is more appropriate for rheological studies. It should be noted that the data related to the models in which the yield stress is negative or the power index is greater than one have been omitted.

The effect of balango gum concentration on the fit of complex rheological data to mathematical models is shown in Table 8.

**Table 8- Effect of Balangu gum concentration on the fit of nanocomplex rheological data with mathematical models**

Treatments	Indices	Mathematical Models				
		Newtonian	Bingham	Power	Herschel-Bulkley	Sisko
T1	RMSE	0.0886	-	-	-	-
	$r^2$	0.998	-	-	-	-
	SSE	0.0035	-	-	-	-
T2	RMSE	0.1885	0.7151	0.1885	0.0461	0.9211
	$r^2$	0.988	0.983	0.982	0.939	0.982
	SSE	1.143	1.365	1.549	0.2137	1.640
T3	RMSE	0.8456	10.196	0.1143	0.1052	0.1081
	$r^2$	0.847	0.991	0.996	0.993	0.997
	SSE	6.52	1.930	0.6539	0.5452	0.6091

As can be seen from the results in Table 8, for samples containing sodium caseinate and 0% balangu gum, the Newtonian model had the highest coefficient related to  $r^2$  and the lowest coefficient related to SSE. In the sample containing 0.25% balangu gum, the Newtonian model had the highest coefficient related to SSE and the lowest to RMSE, the Bingham model had the highest coefficient related to SSE and the lowest to RMSE, the Tavan model had the highest coefficient related to SSE and the lowest to RSME, the Herschel-Balkely model had the highest coefficient related to SSE and the lowest to RMSE, and the Cisco model had the same. In the complex containing 0.5% of balangu gum, in the Newtonian law, the highest coefficient was related to SSE and the lowest to RMSE, in the Bingham law, the lowest coefficient was related to SSE and the highest to RMSE, and in the power law model, the lowest coefficient was related to SSE and the highest to RSME, in the Herschel-Bulkley model, the highest coefficient was related to  $r^2$  and the lowest to RMSE, and in the Cisco model, the same was true.

The results of fitting the power law, Herschel-Bulkley and Cisco models in the sample containing 0% of balango gum and sodium caseinate (0.5%) show that the complex containing sodium caseinate showed Newtonian behavior. Increasing the concentration of balangu gum in these types of complexes caused the behavior to change to non-Newtonian and Herschel-Bulkley type. Given that the structural form of the protein in acidic conditions, intermolecular bonds and thermodynamic properties of the protein determine the type of interaction between particles and the rheological behavior of the system, such behavior was observed as a result [27].

### 3-7- Effect of Balangu gum concentration on apparent viscosity and variables of Newton's and Herschel-Bulkley's models

The indices related to the specified flow behavior models are given in Table 9. This table also shows the apparent viscosity of the sodium caseinate and Balangu gum complex samples at a shear rate of 100 1/s and a temperature of 10°C.

**Table 9 - Effect of Balangu gum concentration on apparent viscosity and variables of Newtonian and Herschel-Bulkley 's model**

Treatments	Apparent viscosity ((mPa.s)	Consistency coefficient (k)	Power index (n)	Yield stress $\sigma_0$ (mPa)
T1	5.12	-	-	-
T2	17.90	0.0018	0.9366	1.351
T3	31.45	0.1056	0.7222	2.123

As can be seen from Table 9, increasing the concentration of balangu gum to sodium caseinate has caused an increase in viscosity. Other studies have indicated an increase in the viscosity of various complexes due to the addition of different hydrocolloids [28].

The increase in viscosity can be attributed to the formation of electrostatic bonds and the creation of a network. With increasing concentration, there is a possibility of forming more bonds and a stronger network, which will increase the viscosity as more water is confined in the network [29]. Also, considering the water absorption capacity of balangu gum polysaccharides, it can be said that the absorption of more water due to increasing concentration will also cause an increase in viscosity. Basically, concentration is one of the variables whose increase or decrease causes a change in the viscosity.

The increase in the viscosity of complexes with increasing gum concentration can be attributed to the creation of a network that has a structure. In this way, the possible role of intermolecular and intramolecular reactions and overlap of balangu gum polysaccharides in increasing viscosity is determined and it can be said that the occurrence of these reactions is probably due to the presence of side branches in the gum structure [6].

Viscosity introduces one of the most important parameters in the preparation of biopolymer complexes. In the study of Ghasemi et al. (a2017), the lowest viscosity was reported at acidic pHs. At higher pHs (6 and 9), the viscosity was higher and lower than pH 3, respectively. At pH 6, whey protein concentrate and pectin were able to form co-

soluble complexes that were able to retain more water and thus increase viscosity. At pH 9, the repulsion between the two polymers was greater and, as a result, the viscosity decreased with less water retention. The higher the probability of complex formation, the lower the viscosity and stability. Therefore, there is an indirect relationship between complex formation and stability/viscosity. In other words, when the probability of complex formation is low, the zeta potential of the biopolymers used is similar and high, which will lead to the creation of a driving force and higher stability/viscosity of the nanocomplex particles [29].

### 8-3- Results of Infrared Spectroscopy (FTIR) of Sodium Caseinate and Balangu Gum Complex

Infrared spectroscopy enables the identification of the main chemical groups in polysaccharides and proteins and the change and formation of new interactions because the wave number and intensity of bonds and groups are specific for each polysaccharide and protein [10]. Considering that functional groups and different bonds have absorption at certain wave numbers (frequencies), the creation of new interactions and changes in the structure of materials cause changes in the absorption wave numbers; therefore, infrared spectroscopy is a suitable tool for detecting and displaying structural changes in materials. In this study, infrared spectroscopy analysis was used to identify functional groups in the sodium caseinate and gum balangu complex (at an equal amount of 0.5%). The resulting graph is shown in Figure 3.

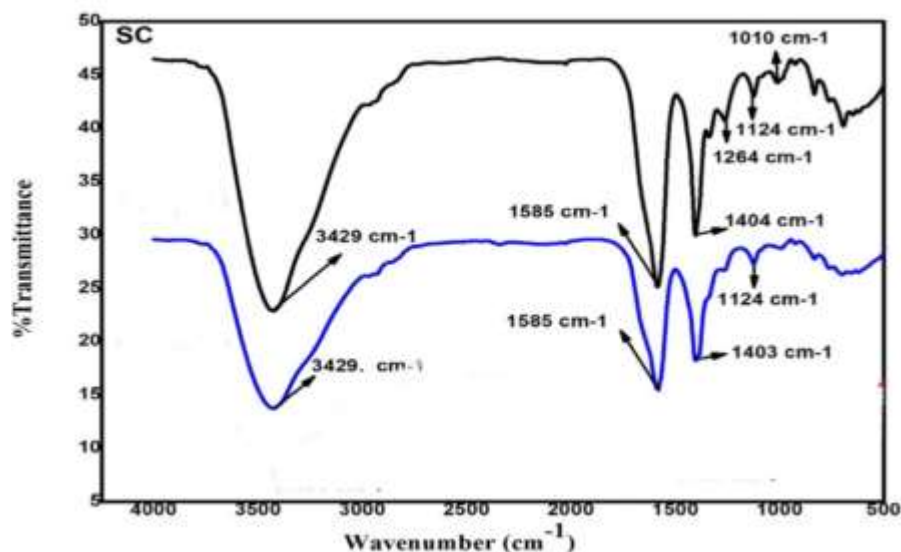


**Figure 3 - The graph obtained from the FTIR infrared spectrogram, the blue lines are related to sodium caseinate and the black lines are related to the caseinate and gum balangu complex (0.5%).**

In the FTIR diagram of sodium caseinate, peaks were observed at wavenumbers of 3429, 1585, 1404, 1264, 1124 and 1010  $\text{cm}^{-1}$ . In the complex containing 0.5% sodium caseinate and 0.5% balangu gum, peaks were also observed at wavenumbers of 3429, 1585, 1403 and 1124  $\text{cm}^{-1}$ . The spectra of the complex of sodium caseinate and balangu gum showed a bandwidth in the spectral region of 3000-3500  $\text{cm}^{-1}$  due to the overlap of free and bound O-H of polysaccharides with N-H groups of protein. Balangu gum consists of hemicellulose compounds, protein macromolecules and sugars that provide -NH<sub>2</sub>, -COOH and -OH functional groups. The addition of gum to the caseinate protein complex helps in the formation of more functional groups to form intermolecular H bonds with the protein, resulting in a wider -OH band. Due to the hydrophilic nature of gum balangu, the high moisture content is also responsible for the wider -OH band [30]. By adding gum to sodium caseinate, the OH peak shifted from 3429  $\text{cm}^{-1}$  to 3430  $\text{cm}^{-1}$ , which is related to the strong interaction between protein and gum. The decrease in the intensity

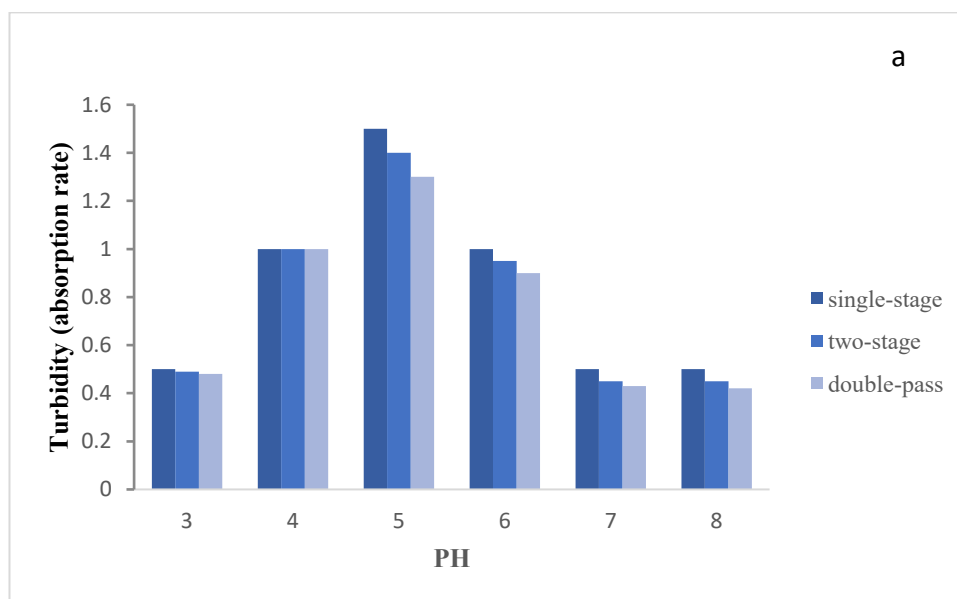
of other bands at 1264  $\text{cm}^{-1}$ , 1334  $\text{cm}^{-1}$  and 700-1000  $\text{cm}^{-1}$  was due to the addition of gum balangu (0.5%), which resulted in structural modification in sodium caseinate and strongly indicated the intermolecular interaction with gum. In addition, a broader band at 1403  $\text{cm}^{-1}$  with the incorporation of gum balangu could be related to the increase of carboxylate group from protein and uronic acid present in the gum structure [31]. Gum balangu shows absorption at wavenumbers of 990-1150  $\text{cm}^{-1}$ , which is related to the stretching of O-C and C-O-C bonds, and the observation of a band at wavenumbers of 1600  $\text{cm}^{-1}$  is related to the presence of free carboxyl groups. As mentioned, these peaks are different in gum and in caseinate, which is of protein nature, and in the complex between these two (protein and polysaccharide), the formed bands indicate other functional groups.

Sardarodiyani et al. studied the FTIR of balangu gum and stated that the absorption at wavenumbers of 1400 and 1600  $\text{cm}^{-1}$  is related to the symmetric and asymmetric C=O stretching of uronic acid, respectively. The

absorption at wavelengths of 1600 to 1700 cm- and 1600 -1500 to 1600 is due to the first amide (CN and C=O group) and the second amide (mainly NH), respectively. The absorption of OH stretching is due to intermolecular and intramolecular hydrogen bonds, which creates a broad absorption region between 3000 and 3500 cm- and shows transitional features, including Free hydroxyl groups that occur in the vapor phase of the samples and show the O-H bond [32].

### 3-9- Effect of homogenization type and pressure on the turbidity of sodium caseinate complex and balangu gum at different pH

The effect of homogenization type on the turbidity of sodium caseinate complex (0.5%) and balangu gum (0.5%) at different pH is shown in Figure 4.



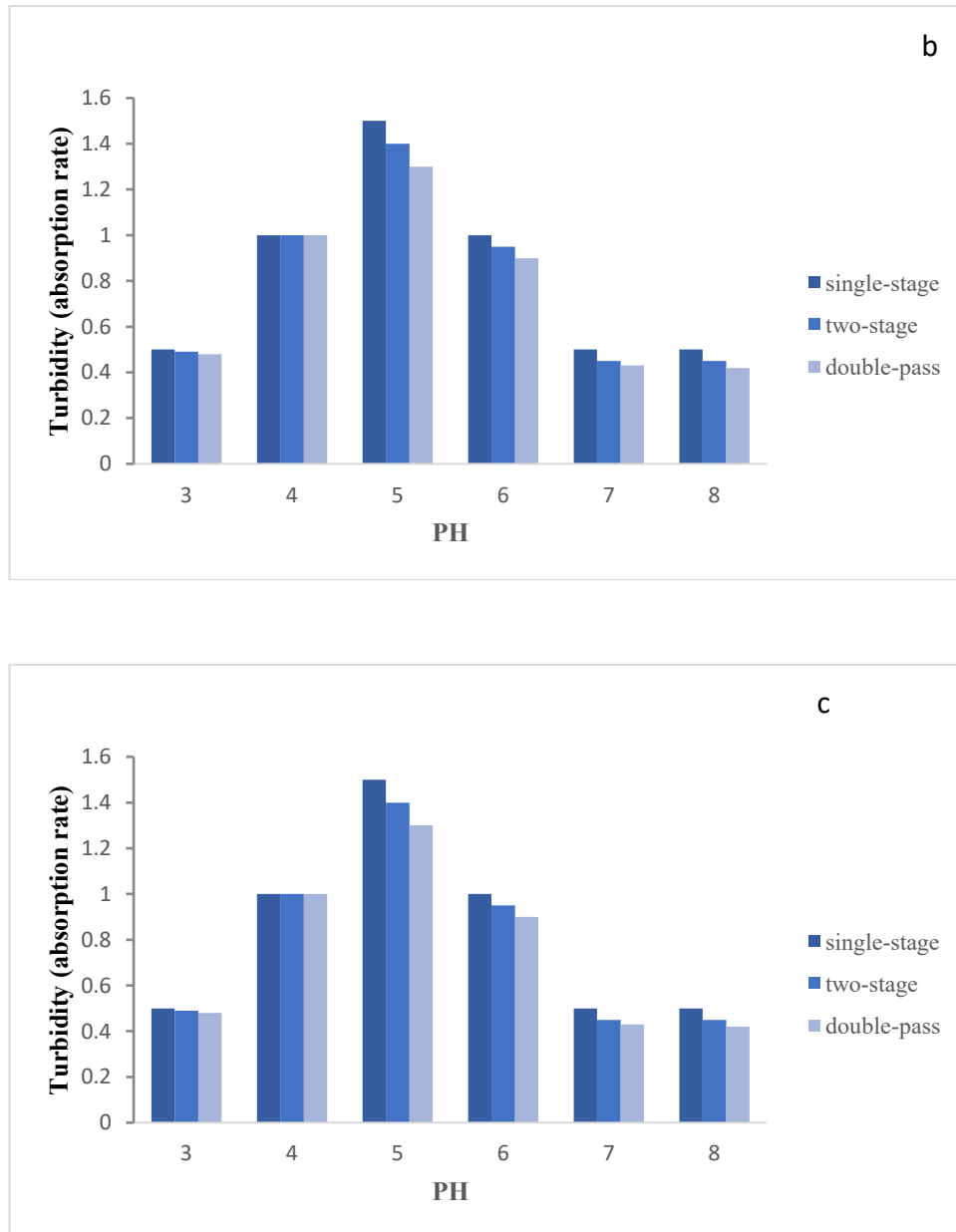


**Figure 4 - Effect of type and amount of pressure [300(a), 500 (b) and 700 (b) bar] of homogenization on the turbidity (absorption) of sodium caseinate and balangu gum complex**

According to Figure 4, in all the pHs studied 3, 4, 5, 6, 7 and 8, the lowest turbidity (absorption) was related to pH 3, followed by pH 7 and 8. The highest turbidity (absorption) was observed in all three pressures studied (300, 500 and 700 bar) and in all three types of homogenization (one-stage, two-stage and double-pass) at pH 5 and then at pH 6.

According to the resulting graphs, the turbidity at each pH studied and at each homogenization pressure is related to the complex sample under single-stage homogenization and the lowest turbidity is related to the sample under 2-pass homogenization. In other words, it can be said that the lowest turbidity (absorption) is related to the sodium caseinate and gum balangu

complex sample under double-pass homogenization and 500 bar pressure at pH 3.

### 3-10- Effect of pressure and type of homogenization on the turbidity of sodium caseinate and balangu gum complex at pH 3.5

According to the results obtained, the production of the complex with 0.5% sodium caseinate and 0.5% gum balangu obtained

better results than the complex containing 0 and 0.25% gum balangu. Therefore, the effect of homogenization pressure and type of homogenization (one-stage, two-stage and double-pass) on the properties of the complex was tested. Table 10 shows the results of the effect of pressure and type of homogenization on the turbidity of the sodium caseinate (0.5%) and gum balangu (0.5%) complex at a pH of 3.5.

**Table 10- Turbidity (absorption rate) of sodium caseinate complex (0.5%) and gum balangu (0.5%) at pH 3.5 and different pressures and types of homogenization**

Pressure (bar)	300	500	700
Type of Homogenization			
Single-stage	0.86±0.2 <sup>Aa</sup>	0.70±0.5 <sup>Ba</sup>	0.55±0.1 <sup>Ca</sup>
Two-stage	0.73±0.1 <sup>Aab</sup>	0.65±0.2 <sup>Bab</sup>	0.51±0.09 <sup>Cab</sup>
Double-pass	0.70±0.3 <sup>Ab</sup>	0.60±0.1 <sup>Bab</sup>	0.48±0.3 <sup>Cab</sup>

Different uppercase letters in each row indicate significant differences between amount of pressures and different lowercase letters in each column indicate significant differences at different type of homogenization ( $p < 0.05$ ).

According to the results of Table 10, the type of homogenization and the homogenization pressure have a statistically significant effect on the absorption and turbidity of the sodium caseinate and gum balangu complex in some samples ( $p < 0.05$ ). At a pressure of 300 bar, there is no statistically significant difference between the turbidity of the complex samples under one-stage and two-stage homogenization. There is also no significant difference between the turbidity of the sample under two-stage and double -pass homogenization. At a pressure of 500 bar, there is no statistically significant difference between the turbidity of the complex samples ( $p > 0.05$ ). At a pressure of 700 bar, there is no statistically significant difference between the turbidity of the complex samples under single-stage and two-stage homogenization. There is also no significant difference between the turbidity of the sample under two-stage and double-pass homogenization.

Regarding the type of homogenization, in single-step homogenization, the sample has higher turbidity and absorption, and the lowest turbidity is related to the sample that has undergone double-pass homogenization. Considering the homogenization pressure, it can be concluded that with increasing pressure in each type of homogenization under study, the turbidity and absorption decrease, and this decrease is significant ( $p < 0.05$ ). Therefore, the lowest turbidity is related to the sample that has undergone double-pass homogenization at a pressure of 700 bar.

### 3-11- Results of the effect of pressure and type of homogenization on the particle size of sodium caseinate complex and gum balangu at pH 3.5

Table 11 shows the results of the effect of pressure and type of homogenization on the particle size of sodium caseinate complex (0.5%) and gum balangu (0.5%) at pH 3.5.

**Table 11- particle size (nm) of sodium caseinate complex (0.5%) and gum balangu (0.5%) at pH 3.5 and different pressures and types of homogenizations**

Pressure (bar)	300	500	700
Type of Homogenization			
Single-stage	611.66±5.1 <sup>Aa</sup>	540.10±5.2 <sup>Ba</sup>	450.50±5.5 <sup>Ca</sup>
Two-stage	601.66±2.7 <sup>Aab</sup>	520.15±4.3 <sup>Bb</sup>	433.33±3.2 <sup>Cab</sup>
Double-pass	583.33±2.2 <sup>Ac</sup>	498.33±4.1 <sup>Bc</sup>	396.66±2.6 <sup>Cc</sup>

Different uppercase letters in each row indicate significant differences between amount of pressures and different lowercase letters in each column indicate significant differences at different type of homogenization ( $p \leq 0.05$ ).

According to the results of Table 11, at a pressure of 300 bar, there is a significant difference ( $p < 0.05$ ) between the particle sizes of the complex samples under different homogenizations. At a homogenization pressure of 300 bar, the largest particle size is related to the sample under single-stage homogenization and the smallest particle size is related to the sample under double-pass homogenization. At a pressure of 500 bar, there is also a significant difference between the particle sizes under single-stage homogenization and the sample under double-stage homogenization, as well as between the particle sizes of the sample under two-stage homogenization and the sample under double-pass homogenization. At this pressure, the smallest particle size is related to the sample under double-pass homogenization and the largest particle size is related to the sample under single-stage homogenization. At a pressure of 700 bar, there is no significant difference between the particle size of the sample subjected to single-stage homogenization and the sample subjected to two-stage homogenization ( $p > 0.05$ ), but this difference between these samples and the sample subjected to double-pass homogenization is significant ( $p < 0.05$ ). Regarding the type of homogenization, with increasing pressure in all the homogenizations studied, the particle size decreases, and there

is a significant difference between the particle size in the samples under each homogenization at different pressures ( $p < 0.05$ ). The smallest particle size is related to the sample subjected to double-pass homogenization at a pressure of 700 bar.

### 3-12-Results of the effect of pressure and type of homogenization on the zeta potential of sodium caseinate and balangu gum at pH 3.5

Zeta potential indicates the net surface charge of microcapsules. Increasing the zeta potential increases the stabilization of colloidal systems due to the increase in electrostatic repulsion forces. The high zeta potential of the emulsion particles increases the electrostatic repulsion force and, as a result, increases the physical stability of the system. Several factors, including ionic strength, type and concentration of polysaccharide macromolecules, their ratio, pH, etc., affect the amount of surface charge, electrophoretic mobility, and zeta potential [10]. Table 12 shows the results of the effect of pressure and type of homogenization on the zeta potential of sodium caseinate complex (0.5%) and balangu gum (0.5%) at a pH of 3.5.

**Table 12- Zeta potential (mv) of sodium caseinate complex (0.5%) and gum balangu (0.5%) at pH 3.5 and different pressures and types of homogenizations**

Pressure (bar)	300	500	700
Type of Homogenization			
Single-stage	-19.66 <sup>Ab</sup>	-24.33 <sup>Ba</sup>	-30.00 <sup>Cb</sup>
Two-stage	-15.33 <sup>Aa</sup>	-24.66 <sup>Ba</sup>	-24.66 <sup>Ba</sup>
Double-pass	-24.66 <sup>Ac</sup>	-27.64 <sup>Aa</sup>	-35.33 <sup>Bc</sup>

Different uppercase letters in each row indicate significant differences between amounts of pressures and different lowercase letters in each column indicate significant differences at different type of homogenization ( $p \leq 0.05$ ).

According to the data in Table 12, at a pressure of 300 bar, there is a significant difference ( $p < 0.05$ ) between the zeta potential of the complex samples under different homogenizations. At a homogenization pressure of 300 bar, the highest negative zeta potential was related to the sample under double-pass homogenization and the lowest was related to the sample under two-stage homogenization. At a pressure of 500 bar, there was no significant difference between the negative zeta potential under single-stage homogenization, the sample under two-stage homogenization, and the sample under two-pass homogenization. At this pressure, the highest negative zeta potential was related to the sample under double-pass homogenization and the lowest was related to the sample under one-stage homogenization. At a pressure of 700 bar, there was a significant difference between the negative zeta potential of the sample subjected to single-stage homogenization, the sample subjected to two-stage homogenization, and the sample subjected to double-pass homogenization

( $p < 0.05$ ). Regarding the type of homogenization, with increasing pressure in all homogenizations studied, the negative zeta potential increased. The highest negative zeta potential was related to the sample subjected to double-pass homogenization at a pressure of 700 bar. Increasing the molecular weight of the nanocomplex also causes the zeta potential to become more negative in the emulsions. Since the isoelectric pH of sodium caseinate is approximately equal to 5 and the pH of the solutions is considered to be 3.5, the zeta potential becomes negative.

### **3-13-Effect of homogenization type and pressure on the rate of shear stress changes in sodium caseinate complex and balangu gum**

The effect of homogenization type and pressure on the rate of shear stress changes (pa) in sodium caseinate complex (0.5%) and balangu gum (0.5%) at different shear rates is shown in Figure 5.

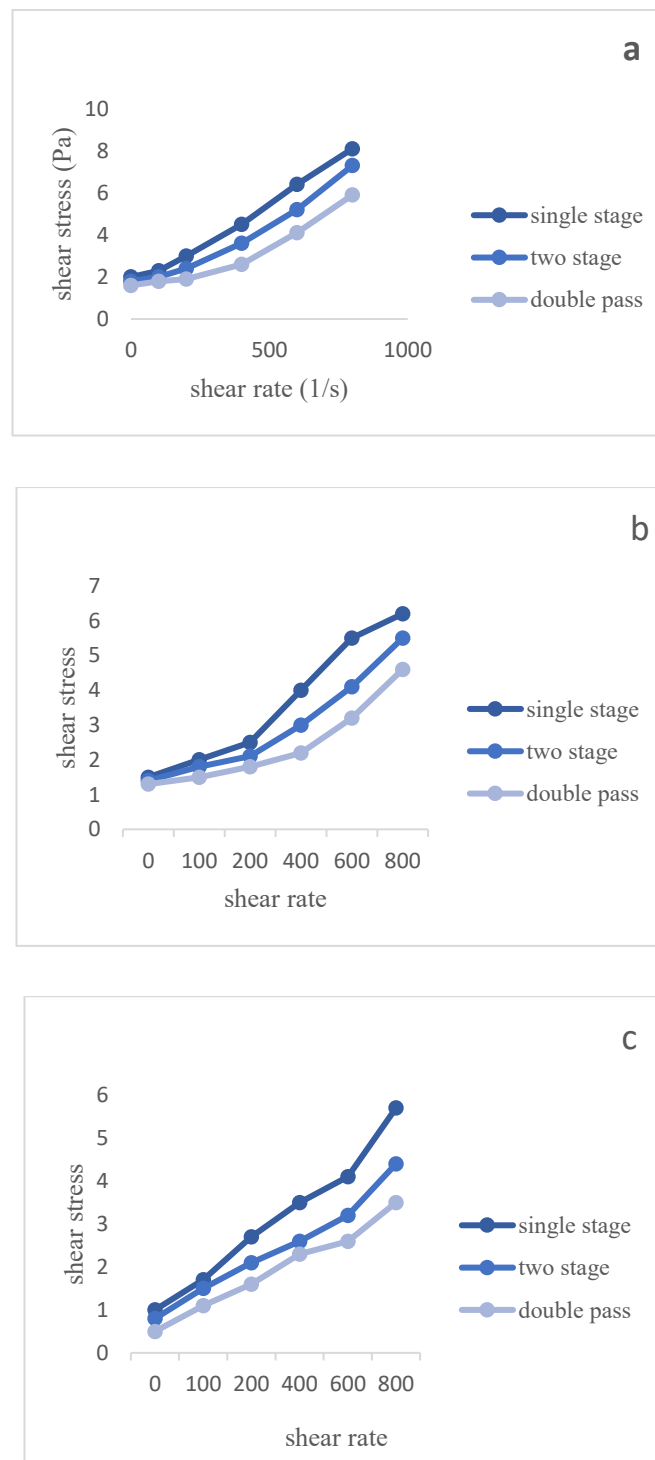


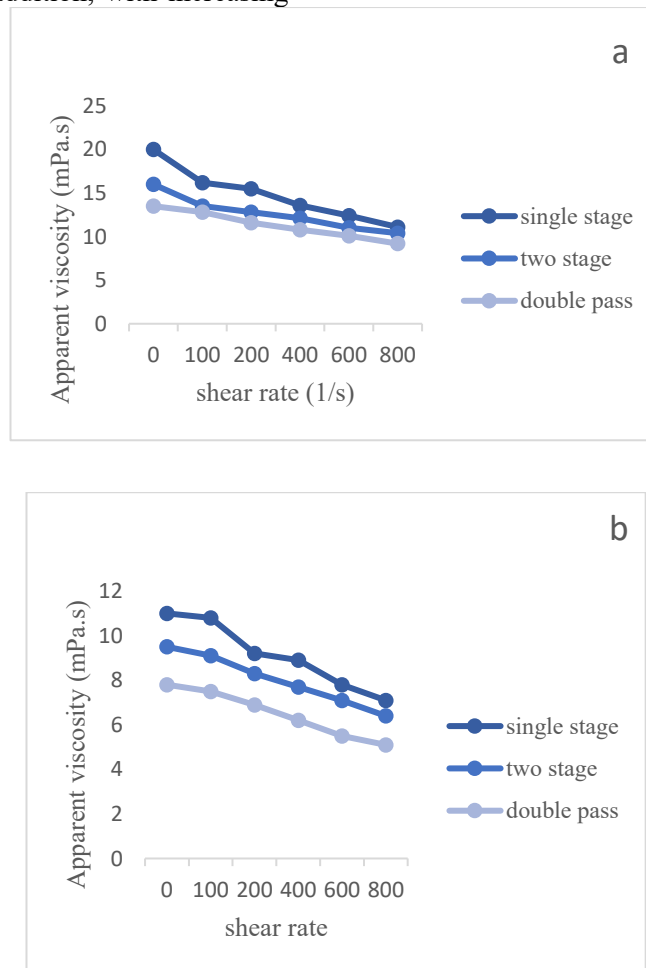
**Figure 5 - Effect of type and pressure [300(a), 500(b) and 700 (c) bar] of homogenization on the shear stress of sodium caseinate and gum balangu complex at different shear rates**

According to the data in Figure 5, at all homogenization pressures of 300, 500 and 700 bar, with increasing shear rate, the shear stress also increased and the highest shear stress in all three types of single-stage, two-stage and double-pass homogenization was related to the complex samples that were subjected to a shear stress of 800 1/s. In fact, a linear relationship can be obtained between the shear rate and shear stress. The lowest shear stress in all three pressures of 300, 500 and 700 bar was related to the complex sample under no shear rate. At each shear rate, the highest stress was related to the sample under single-stage homogenization and the lowest value was related to the sample under double-pass homogenization. In addition, with increasing

homogenization pressure, the rate of shear stress changes was less compared to different shear rates, meaning that the lowest shear stress was observed in the double-pass homogenization type at a pressure of 700 bar.

### 3-14- Effect of homogenization type and pressure on the apparent viscosity of sodium caseinate complex and balangu gum

The effect of homogenization type and pressure (300, 500 and 700 bar) on the apparent viscosity (millipascals) of sodium caseinate complex (0.5%) and balangu gum (0.5%) at different shear rates is shown in Figure 6.



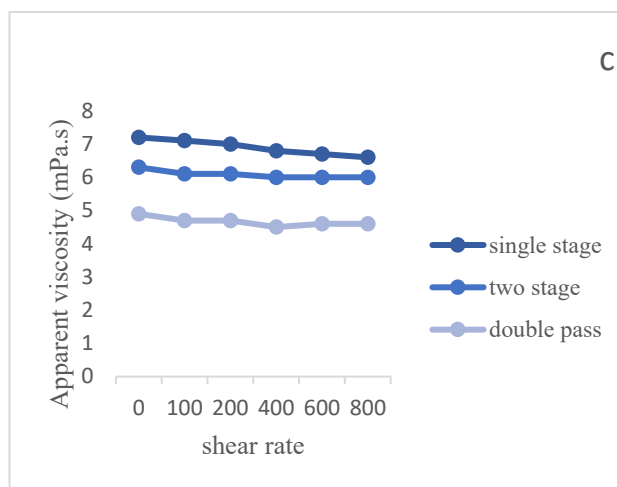


**Figure 6 - Effect of type and pressure [300(a), 500(b) and 700 (c) bar] of homogenization on the apparent viscosity of sodium caseinate and gum balangu complex at different shear rates**

According to the results of Figure 6, at a pressure of 300 bar, with increasing shear rate, viscosity decreased. At a pressure of 500 bar, no difference was observed between the viscosity of the complex sample under shear rates of 0, 100 and at 700 bar under shear rates of 0, 100 and 200, especially in the sample under double-pass homogenization. At the remaining shear rates studied, the viscosity also decreased in each sample with increasing shear rate. In the samples under single-step homogenization at each shear rate studied and at each pressure used, the complex samples had lower viscosity than the complex samples under double-pass and two-stage homogenization, and the sample under double-pass homogenization had higher viscosity than the other samples. The highest viscosity also corresponds to the pressure of 700 bar, which had the lowest shear stress versus shear rate.

Viscosity was introduced as one of the most important parameters in the preparation of biopolymer complexes. In the study of Ghasemi et al., the lowest viscosity was reported at acidic pHs. At higher pHs (6 and 9), the viscosity was higher and lower than pH 3, respectively. The higher the probability of complex formation, the lower the viscosity and stability. Therefore, there is an indirect

relationship between complex formation and stability/viscosity. In other words, when the probability of complex formation is low, the zeta potential of the biopolymers used is similar and high, which will lead to higher driving force and stability/viscosity of the nanocomplex particles [29]. According to the results, the studied samples showed shear thinning behavior (pseudoplastic) because with increasing shear rate, the viscosity decreased and the shear stress increased.

Tarighati et al. stated that gums have the ability to stabilize oil-in-water emulsions stabilized with whey protein due to the creation of high viscosity, increased viscosity of the continuous phase, and reduced movement of oil particles, and marjoram seed gum prevents the enlargement of oil-in-water emulsion particles by slowing down the movement of particles due to increased viscosity [33].

### **3-15- The effect of the type and amount of homogenization pressure on fitting the rheological data of the complex sample with mathematical models**

The effect of the type and amount of homogenization pressure on fitting the rheological data of the complex sample with mathematical models is shown in 13.

**Table 13- Effect of type and amount of homogenization pressure on fitting rheological data of complex sample with mathematical models**

Pressure (bar)	Type	Indices	Newtonian	Bingham	Power	Herschel-Bulkley	Sisko
<b>300</b>	Single-stage	RMSE	0.4626	0.1125	0.0713	0.0678	0.0721
		$r^2$	0.925	0.985	0.988	0.989	0.995
		SSE	12.27	0.88	0.405	0.36	0.311
	Two-stage	RMSE	0.3896	0.1296	0.0559	-	-
		$r^2$	0.961	0.995	0.998	-	-
		SSE	7.452	1.039	0.213	-	-
	Double-pass	RMSE	0.3119	0.086	0.0525	0.0531	0.0721
		$r^2$	0.982	0.994	0.996	0.995	0.996
		SSE	4.853	0.1143	0.1564	0.1619	0.311
<b>500</b>	Single-stage	RMSE	0.0825	0.0627	0.0252	0.0262	0.0264
		$r^2$	0.995	0.996	0.995	0.998	0.998
		SSE	0.382	0.225	0.036	0.0425	0.0421
	Two-stage	RMSE	0.0922	0.0225	0.0129	0.0465	-
		$r^2$	0.996	0.997	0.999	0.999	-
		SSE	0.492	0.0348	0.012	0.1249	-
	Double-pass	RMSE	0.0087	0.0119	0.0132	0.0140	-
		$r^2$	0.998	0.988	0.996	0.994	-
		SSE	0.0043	0.0083	0.0103	0.0114	-
<b>700</b>	Single-stage	RMSE	0.053	0.0255	0.0151	-	-
		$r^2$	0.998	0.996	0.998	-	-
		SSE	0.1657	0.0377	0.0137	-	-
	Two-stage	RMSE	0.0091	0.0095	-	-	-
		$r^2$	0.994	0.995	-	-	-
		SSE	-	-	-	-	-

	SSE	0.0022	0.061	-	-	-
	RMSE	0.0061	0.0135	-	-	-
Double-pass	$r^2$	0.993	0.997	-	-	-
	SSE	0.249	0.0251	-	-	-

According to the results of Table 14, the  $r^2$  of the sodium caseinate and balangu gum complex (0.5%) is shown in the table. At a pressure of 300 bar in the single-stage homogenization method, the Cisco model, followed by the Tavan and Herschel-Bulkley models, have higher  $r^2$ , and since the Herschel-Bulkley coefficient is less than 1, it indicates shear-diluting behavior. At a pressure of 300 bar in the two-stage homogenization method, the highest  $r^2$  is related to the Power model, and in the two-pass homogenization method, the highest  $r^2$  is related to the Cisco model and then Tavan. At a pressure of 500 bar, the  $r^2$  is also higher than the other coefficients in the different models, and the  $r^2$  in the single-stage homogenization method is higher in the Herschel-Bulkley and Cisco models, and since it is less than one, it confirms the shear-diluting behavior. At a pressure of 500 bar in the two-stage homogenization method, the  $r^2$  of the models under study is high but less than one, which, as stated, indicates shear thinning behavior. At a pressure of 500 bar and the two-pass homogenization method, the highest  $r^2$  is related to the Herschel-Bulkley, Power, and Newtonian models, and they are less than one. At a pressure of 700 bar in the single-stage homogenization method, the highest  $r^2$  is related to the Herschel-Bulkley and Power models, and in the two-stage homogenization method and the two-pass method, the highest  $r^2$  is related to the Bingham model. In all cases under study, the  $r^2$  was high and the RMSE was low, which indicates pseudoplastic behavior in the complex samples [34].

Nik Nam et al. investigated the stable and dynamic rheological properties of emulsions containing plantain seed gum extracted by ultrasonic pretreatment. According to the results of these researchers, all the models studied had high  $r^2$  (0.97-1) and low RMSE (0.0046-6.085). Based on the power law, all the emulsions studied showed shear-fluidity behavior, which can be inferred from the flow index values, which were less than 1 in all samples. Also, in their results, by increasing the gum content from 0.3% to 1% w/v, the flow index values decreased from 0.810 to 0.661. In the study of these researchers, by increasing the amount of gum from 0.3% to 1% w/v, the values of the consistency coefficient increased, and higher values of the consistency coefficient could be related to the molecular weight, because the molecular weight values play a very important role in the viscosity of gum solutions and emulsions containing them [35]. The results of previous research by Naji-Tabasi showed that for fitting the shear stress-shear rate data of emulsions containing basil seed gum, the Herschel-Bulkley model was the most appropriate model due to its R of 0.99 and RMSE less than 0.42 [36]. Samavati et al. investigated the shear stress-shear rate of emulsions containing tragacanth gum and selected the power law as the most appropriate model for fitting [37]. According to the results of fitting the shear stress-shear rate data in the present study, it was shown that the Herschel-Bulkley model is the most appropriate model for fitting these data due to its  $r^2$  values less than one and low RMSE.

Since the optimal pH is considered to be 3.5, it can be said that at acidic pH, the neutralization of the negative charges of

casein affects the degree of attraction and intermolecular bonds and affects the rheological properties.

Mohammad Khusht Chin et al. used basil seed gum to encapsulate grapefruit peel essential oil and observed shear thinning (pseudoplastic) behavior in the microencapsulated samples at homogenization cycles of 10,000, 15,000, and 20,000 rpm. In their study, the models described the flow behavior of encapsulated essential oils with high  $r^2$ . Time-independent rheological models including Power, Herschel Bulkley, Bingham and Casson showed that Power and Herschel- Bulkley models had higher R than the other models. The flow index value in Power and Herschel- Bulkley models was less than 1, which confirmed the shear thinning behavior of the samples [34].

#### 4-Conclusion

In general, the results showed that for the production of sodium caseinate and gum balangu complex, the best combination was to use 0.5% sodium caseinate, 0.5% gum balangu using a double-pass homogenizer and 700 bar pressure at pH 3.5.

#### Data Availability

The data used to support the finding of this study are available from the corresponding author upon request.

#### Conflict Of Interest

The authors have no conflicts interest to report.

#### Funding Statement

The researchers did not receive any specific grant from funding agencies the public, commercial or not-for-profit sectors.

#### 5-References

[1] Jones, O., Andrew, E. D. & McClements, D. J. 2010. Thermal analysis of b-lactoglobulin complexes with pectin or carrageenan for

production of stable biopolymer particles. *Food Hydrocolloids*, 24: 239–248.

[2] Salehi, F., & Kashaninejad, M. 2014. Effect of Different Drying Methods on Rheological and Textural Properties of Balangu Seed Gum, *Drying Technology*. 32: 720-727.

[3] Salehi, F., Kashaninejad, M., & Behshad, V. 2014. Effect of sugars and salts on rheological properties of Balangu seed (*Lallemantia royleana*) gum, *International Journal of Biological Macromolecules*. 67,16-21

[4] Anal, A. K., Tobiassen, A., Flanagan, J. & Singh, H., 2008, Preparation and characterization of nanoparticles formed by chitosan–caseinate interactions, *Colloids and Surfaces B: Biointerfaces*, 64: 104–110.

[5] Ghosh, A., & Bandyopadhyay, P. 2012. Polysaccharide–protein complexes and their applications. *Carbohydrate Polymers*, 89(4): 1310–1316.

[6] Mohammadi, S. 2019. Production of tragacanth/whey protein nanocomplex for curcumin encapsulation and simulation of rheological properties and its release in the model system and pasteurized dairy dessert. PhD thesis. Gorgan University of Agricultural Sciences and Natural Resources.

[7] Ghasemi, S., Jafari, S. M., Assadpour, E. & Khomeiri, M. 2017a. Production of pectin-whey protein nano-complexes as carriers of orange peel oil. *Carbohydrate Polymers*, 177: 369-377.

[8] Eghbal, N., Yarmanda, M. S., Mousavia, M., Degraevb, P., Oulahalb, N. & Gharsallaouib, A. 2016. Complex coacervation for the development of composite edible films based on LM pectin and sodium caseinate. *Carbohydrate Polymers*. 151: 947-956.

[9] Azarikia, F. & Abbasi, S. 2015. Efficacy of whey protein–tragacanth on stabilization of oil-in-water emulsions: Comparison of mixed and layer-by-layer methods. *Food Hydrocolloids*. 2: 1-34.

[10] Khoshmanzhar, M., Ghanbarzadeh, B., Hamishekar, H., Saati Khiabani, M. & Rezaei Makram, R. 2012. Investigation of factors affecting particle size, zeta potential and rheological properties of the paste in a colloidal system containing kappa-carrageenan-sodium

caseinate nanoparticles. Research and Innovation in Food Sciences and Industries. 1 (4): 255-272.

[11] Azizanbari, C., Ghanbarzadeh, B., Hamishehkar, H., & Hosseini, M. (2019). Gellan - Caseinate Nanocomplexes as a Carrier of Omega-3 Fatty Acids: study of Particle size, Rheological Properties and Encapsulation Efficiency. Food Processing and Preservation Journal, 5 (2): 19-42.

[12] Khoshmanzar, M., Ghanbarzadeh, B., Hamishehkar, H., Sowti, M., & Hoseini, M. (2014). Sodium Caseinate-Carrageenan Biopolymeric Nanocomplexes as a Carrier of Vitamin D: Study of Complex Formation, Particles Size and Encapsulation Efficiency. Iranian Journal of Polymer Science and Technology, 27(1): 37-49.

[13] Jourdain, L., Leser, M. E., Schmitt, C., Michel, M. & Dickinson, E. 2008. Stability of emulsions containing sodium caseinate and dextran sulfate: relationship to complexation in solution. Food Hydrocolloids. 22: 647-659.

[14] Gorji, S.G., Gorji, E.G., & Mohammadifar, M.A. 2014. Characterisation of gum tragacanth (*Astragalus gossypinus*)/sodium caseinate complex coacervation as a function of pH in an aqueous medium. Food Hydrocolloids, 34:161-168.

[15] Ru, Q., Wang, Y., Lee, J., Ding, Y., & Huang, Q. 2012. Turbidity and rheological properties of bovine serum albumin/pectin coacervates: effect of salt concentration and initial protein/polysaccharide ratio. Carbohydrate Polymers, 88(3): 838-846.

[16] Ye, A., Flanagan, J., & Singh, H. 2006. Formation of stable nanoparticles via electrostatic complexation between sodium caseinate and Arabic gum. Biopolymers, 82(2): 121-133.

[17] Kobori, T., Matsumoto, A., & Sugiyama, S. 2009. pH-Dependent interaction between sodium caseinate and xanthan gum. Carbohydrate Polymers, 75(4): 719-723

[18] Girard, M, Turgeon, S. L. & Gauthier, S. F. 2004. Thermodynamic parameters of beta-lactoglobulin -pectin complexes assessed by isothermal titration calorimetry. Journal of Agriculture Food Chemistry. 51: 4450-4455.

[19] Zhou, X., Guo, N., Zhang, F., Zhuo, K., & Zhu, G. 2024. Improving stability and bioavailability of ACNs based on Gellan gum-

wehy protein isolate nanocomplexes. Food Chemistry, X, 24, 102050.

[20] Karim, A., Rehman, A., Jafari, S. M., Miao, S., Dabbour, M., Ashraf, W., & Lianfu, Z. 2024. Fabrication and Characterization of Sonicated Peach Gum-Sodium Caseinate Nanocomplexes: Physicochemical, Spectroscopic, Morphological, and Correlation Analyses. Food and Bioprocess Technology, 18(3):2462-2481.

[21] Akrami, M., Ghanbarzadeh, B., Pourzafar, F., Mortazavi, A., Dinarvand, R., & Dehghannia. J. 2016. Gum Arabic-Caseinate Nanocomplexes Carrying Beta-Carotene (2): Investigation of Particle Size, Zeta Potential, Morphology and Encapsulation Efficiency. Food Industry Research, 26(4): 763-778.

[22] GBassi, G., Yolou, F., Sarr, S., Atheba, P., Amin, C. & Ake, M. 2012. Whey protein analysis in aqueous medium and in artificial gastric and intestinal fluids. International Journal of Biological and Chemical Sciences, 6: 1828-1837.

[23] Ranjit, K. & Baquee, A. A. 2013. Nanoparticle: an overview of preparation, characterization and application. International research journal of pharmacy, 4 (4): 47-57.

[24] Rasheed, H. A., Rehman, A., Li, C., Bai, M., Karim, A., Dai, J., & Lin, L. 2024. Fabrication of Citrus bergamia essential oil-loaded sodium caseinate/peach gum nanocomplexes: Physicochemical, spectral, and structural characterization. International Journal of Biological Macromolecules, 260: 129475.

[25] Nowrouzi S, Ghods Rohani M, Rashidi H. 2021. Effects of Balangu Seed Gum on Physicochemical and Sensory Characteristics of Low-Fat Fresh Yoghurts. Iranian Journal of Nutrition Science and Food Technology, 16 (2) :69-78

[26] Najaf Najafi M., & Fazeli, A. 2016. Evaluation of Lepidium sativum seed gum effect on physical stability and flow properties of oil-in-water emulsion prepared by high-speed dispersing. Journal of food science and technology, 14 (64) :126-116

[27] Kiani, H., Mousavi, S. M. A. & Emam-Djomeh, Z. 2008. Rheological properties of Iranian yoghurt drink, Doogh. International Journal of Dairy Science, 3: 71-78.

- [28] Chen, B., Li, H., Ding, Y. & Suo, H. 2012. Formation and microstructural characterization of whey protein isolate/beet pectin coacervations by laccase catalyzed cross-linking. *LWT- Food Science and Technology*, 47 (1): 31-38.
- [29] Ghasemi, S., Jafari, S. M., Assadpour, E. & Khomeiri, M. 2017a. Production of pectin-whey protein nano-complexes as carriers of orange peel oil. *Carbohydrate Polymers*, 177: 369-377.
- [30] Punia, S., & Dhull, S. B. 2019. Chia seed (*Salvia hispanica* L.) mucilage (a heteropolysaccharide): Functional, thermal, rheological behaviour and its utilization. *International journal of biological macromolecules*, 140: 1084-1090.
- [31] Semwal, A., Ambatipudi, K., & Navani, N. K. 2022. Development and characterization of sodium caseinate based probiotic edible film with chia mucilage as a protectant for the safe delivery of probiotics in functional bakery. *Food Hydrocolloids for Health*, 2(1): 100065.
- [32] Sardarodiyani, M., Arianfar, A., Mohamadi Sani, A., & Naji-Tabasi, S. 2019. Enzymatic purification of Balangu seed (*Lallemantia royleana*) gum and evaluation of its physicochemical and emulsifying properties. *Journal of food science and technology*, 16 (95): 37-51
- [33] Tarighati H., Raftani Amiri, Z., & Esmaeilzadeh kenari R. 2022. Comparison of free and encapsulated extracts of *Mentha pulegium*'s leaves in *Allysum homolocarpum*, chitosan and chitosan- *Allysum homolocarpum* on oxidative stability of soybean oil during 18 days incubation conditions. *Food industry research*, 32(3): 29-60.
- [34] Mohammad Kheshtchin, S. Farahmandfar, R. & Farmani J. 2022. Effect of homogenization on encapsulation of grapefruit (*Citrus paradisi*) peel essential oil with basil seed gum. *Innovative Food Technologies*, 9(3): 223-238.
- [35] Niknam, R., Ayaseh, A., & Ghanbarzadeh, B. 2018. Steady shear flow and dynamic rheology of the emulsions containing ultrasound-assisted extracted *Plantago major* seed gum. *Journal of Food Science and Technology*, 15(83): 281-298.
- [36] Naji-Tabasi, S., & Razavi, S.M.A. 2016. New studies on basil (*Ocimum bacilicum* L.) seed gum: Part 2 – Emulsifying and foaming characterization. *Carbohydrate Polymers*, 149: 140 – 150.
- [37] Samavati, V., Emam-Djomeh, Z., Mohammadifar, M.A., Omid, M., & Mehdinia, A. 2012. Application of rheological modeling in food emulsions. *Iran Journal of Chemistry and Chemical Engineering*, 31 (2): 71–83.



بررسی ویژگی های فیزیکوشیمیایی و رئولوژیکی نانوکمپلکس تهیه شده از کازئینات سدیم و صمغ دانه بالنگو

رقیه عزتی<sup>۱</sup>، لیلا روزبه نصیرایی<sup>۱</sup>، سارا جعفریان<sup>۱</sup>، مسعود دزیانی<sup>۲</sup>، فاطمه شهدادی<sup>۳</sup>

۱- گروه صنایع غذایی، واحد نور، دانشگاه آزاد اسلامی، نور، ایران

۲- گروه صنایع غذایی، واحد گرگان، دانشگاه آزاد اسلامی، گرگان، ایران

۳- گروه صنایع غذایی، دانشکده کشاورزی، دانشگاه جیرفت، جیرفت، ایران

#### چکیده

#### اطلاعات مقاله

هدف از این مطالعه تهیه و تعیین ویژگی های نانوکمپلکس بیوپلیمری حاوی کازئینات سدیم و صمغ دانه بالنگو بود. جهت تولید نانوکمپلکس از میزان ۰/۵ درصد کازئینات سدیم و ۰/۲۵ و ۰/۵ درصد صمغ بالنگو استفاده شد. سه نوع کمپلکس با درصد صمغ بالنگوی متفاوت تولید شده از نظر کدورت، اندازه ذرات، پتانسیل زتا و همچنین تنش برشی و ویسکوزیته و برازش داده های رئولوژیکی مورد بررسی قرار گرفت. نتایج نشان داد، کمپلکس کازئینات سدیم و ۰/۵ درصد صمغ بالنگو به عنوان کمپلکس برتر انتخاب گردید. علاوه بر آن تاثیر نوع هموژنیزاتور (تک مرحله ای، دو مرحله ای و ۲ بار عبور) و فشار هموژنیزاسیون (۳۰۰، ۵۰۰ و ۷۰۰ بار) در pH های ۳، ۴، ۵، ۶، ۷ و ۸ بر میزان کدورت کمپلکس انجام شد. pH انتخاب شده ۳/۵ در نظر گرفته شد و نمونه در pH معادل ۳/۵، تحت تاثیر نوع و فشار هموژنیزاتور قرار گرفته و ویژگی های آن مورد بررسی قرار گرفت. مطابق نتایج، کمترین میزان کدورت (جذب) مربوط به نمونه کمپلکس کازئینات سدیم و صمغ بالنگو تحت هموژنیزاسیون دوبر عبور و فشار ۵۰۰ بار (۰/۴۸) بود. بیشترین پتانسیل منفی زتا، مربوط به نمونه ای است که تحت هموژنیزاسیون دوبر عبور در فشار ۷۰۰ بار قرار گرفته (۳۵/۳۳- میلی ولت) بود. کمترین اندازه ذرات مربوط به نمونه ای است که تحت هموژنیزاسیون دوبر عبور در فشار ۷۰۰ بار (۳۹۶.۶۶ نانومتر) قرار گرفته است. در تمامی موارد مورد بررسی میزان  $I^2$  بالا و میزان RMSE پایین بود که این امر نشان دهنده رفتار سودوپلاستیک در نمونه های کمپلکس می باشد.

#### تاریخ های مقاله :

تاریخ دریافت: ۱۴۰۴/۰۷/۱۹

تاریخ داوری: ۱۴۰۴/۰۹/۱۲

تاریخ پذیرش: ۱۴۰۴/۰۹/۱۵

#### کلمات کلیدی:

نانوکمپلکس،  
صمغ بالنگو،  
کازئینات سدیم،  
ویژگی های رئولوژیکی،  
هموژنیزاسیون.

DOI: 10.48311/fsct.2026.116950.82884

\* مسئول مکاتبات: